

Invited - Airtouch: A Novel Single Layer 3D Touch Sensing System for Human/Mobile Devices Interactions

Li Du¹, ChunChen Liu¹, Adrian Tang¹, Yan Zhang¹, Yilei Li¹, Kye Cheung², Mau-Chung Frank Chang¹

¹EE Dept., University of California, Los Angeles, CA, USA

²Kneron, Inc., San Diego, CA, USA

¹ {dl1989113, chunchenliu, atang, charlesz1112, ylli1986, mfchang}@ucla.edu

² kyec@kneron.com

ABSTRACT

Touchscreen technology plays an important role in the booming mobile devices market. Traditional touchscreen only provides 2D interactions with limited user experience. To overcome these limitations, we propose a novel 3D touch sensing system called the Airtouch system, which can recognize the movement of the finger in a 3-dimensional space. Half of the manufacturing cost is reduced by applying only single layer electrodes in the touch panel design. Moreover, an oscillator based correlated double sampling circuit is implemented as the self-capacitive sensor with bootstrapping technique to reduce inter-channel-coupling effect. Additionally, new algorithm for finger positioning is created with grouping filter invented to reduce system background noise. The demonstrated setup can successfully detect finger movement within a vertical range of 6cm and achieve a horizontal resolution up to 1cm. This system offers great potential in both gesture recognition for small-sized electronics, and advanced human interactive games for TV and mobile device.

Keywords

Mobile Device, Touchscreen, Capacitive Sensing, Gesture, Grouping Filter, Human/Machine Interface

1. INTRODUCTION

The use of smart mobile devices (e.g, smartphones, tablets) has grown rapidly in the past five years and is quickly replacing the traditional personal computer (PC). Compared with PCs, smart mobile devices offer comparable computation power with a much smaller size, lower weight and more user-friendly interactive human/machine interface (HMI). According to a recent market report, there will be 1.4 billion smartphones in use world-wide by 2016 [1]. What is more, the upcoming Internet of Things and wearable health monitoring have also created more opportunities for low power, smaller size, and smart wearable electronic devices (e.g, smart watches). The Fitbit surge, as an example, has

Permission to make digital or hard copies of all or part of this work for personal or classroom use is granted without fee provided that copies are not made or distributed for profit or commercial advantage and that copies bear this notice and the full citation on the first page. Copyrights for components of this work owned by others than the author(s) must be honored. Abstracting with credit is permitted. To copy otherwise, or republish, to post on servers or to redistribute to lists, requires prior specific permission and/or a fee. Request permissions from permissions@acm.org.

DAC '16, June 05-09, 2016, Austin, TX, USA

Copyright held by the owner/author(s). Publication rights licensed to ACM.
ACM 978-1-4503-4236-0/16/06...\$15.00

DOI: <http://dx.doi.org/10.1145/2897937.2901902>

been very popular with young people for health monitoring and entertainment since the day it was announced on the market.

Among these consumer electronics, the touchscreens have been widely used as the main methodology to bridge the human and machine interaction. Traditional touch screen systems are limited to two-dimensional sensing capability – users are required to touch the screen directly for the system to determine finger position. This technology suffers from various disadvantages, including leaving fingerprints on the screen, unresponsiveness to wet hands and a limited accuracy with shrinking device size. Moreover, the limited sensing dimension has also trapped the development of advanced user interactive games. Unlike in large television and monitor type displays where there is sufficient power to support cameras to detect user's hand motion [2], sensing approach in mobile and wearable device is very limited due to their restricted power and area budget. Therefore, it is important to discover a new method of HMI to have a higher efficiency and increased sensing capabilities.

Recognizing the limitations of current mobile devices, we have developed a new single-layer 3D touch sensing system called Airtouch as a new approach for HMI. This system is designed to accommodate the space and battery constraints of mobile device environment by minimizing the required hardware size and power. It provides the ability for a mobile device to detect the human finger position remotely when fingers are hovering above the screen, as shown in Figure 1. The system consists of a low-cost single layer mobile touchscreen, a highly sensitive capacitive sensing circuit as in [3], and a corresponding finger 3D position detection algorithm that can be programmed into the mobile device's application processor (AP).

The main contributions of our work include:

1. Design a new single layer touch panel for 3D touch sensing that reduces the touchscreen manufacturing cost by half compared with regular two-layer touchscreen;
2. Implement a bootstrapped-oscillator-based correlated double sampling (CDS) capacitive sensing circuit that can eliminate electrode coupling effects and enable accurate finger capacitance detection;
3. Propose a grouping filter for 3D touch sensing background noise reduction;
4. Invent a new finger 3D position calculation algorithm and demonstrate the potential usage of the proposed system integrated with mobile devices.

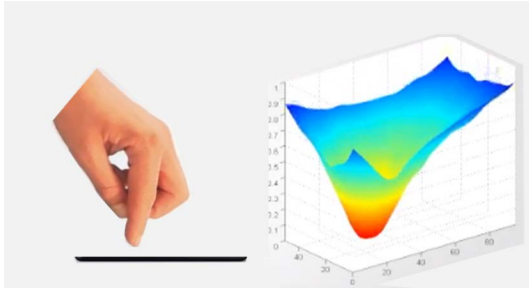


Figure 1: Concept of Airtouch sensing showing non-contact interface using capacitive sensing to determine figure position.

The paper is organized as follows: the hardware design which includes touch panel modeling is described in Section 2. In Section 3, we discuss the corresponding algorithm for finger position estimation. Section 4 reports the performance of this 3D touch sensing system in real-world scenarios. Finally Section 5 outlines the potential applications and concludes the paper.

2. HARDWARE DESIGN

2.1 Touch Panel Design

Current 2D capacitive touch panels are mainly designed with two-layer orthogonal electrodes in order to implement mutual-capacitive sensing [4]. Compared with 2D detection, 3D touch sensing requires the touch panel's electrode to sense a much smaller change in finger capacitance than its own intrinsic parasitic capacitance. This makes the normal two-layer mutual capacitive sensing inapplicable to mobile devices because the large coupling capacitance between electrodes (typically on the order of 30 pF for a 4" mobile device screen) greatly reduces the system sensitivity.

To overcome this, we employ self-capacitance sensing as the methodology to detect the finger-induced capacitance in which the parasitic capacitance will be only the electrode's self-capacitance. Moreover, to reduce the manufacturing cost, a single layer touchscreen is proposed that enables both traditional 2D finger position detection and additional height detection. The touch panel consists of six triangle ITO electrodes deposited on a plastic PET film as shown in Figure 2. Since it is manufactured with one-layer electrodes, fabrication costs are expected to reduce by half compared to traditional two-layer electrode touchscreen.

To evaluate the designed electrode's sensitivity to remote finger position, we use Ansoft Q3D CAD tool to simulate the channel electrode's self-capacitance response versus the height of finger hovering above it. Due to the human body's large form factor, the finger has been modeled as a 10cm-high-grounded cylinder with radius of 0.5cm [5, 6]. The measured self-capacitance of the electrode can be regarded as the summation of the electrode's intrinsic capacitance and the finger-induced capacitance.

As the simulation results show in Figure 3, the designed size of the electrode senses a finger-induced capacitance response of more than 40fF up to 5cm finger height which is large enough for analog circuitry to detect [7]. Moreover, the sweep of the finger in Y direction at the same height shows a comparable difference in the electrode's self-capacitance.

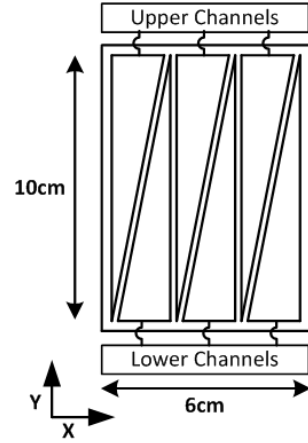


Figure 2: Single-Layer Airtouch panel showing electrode geometry and touchpanel dimensions.

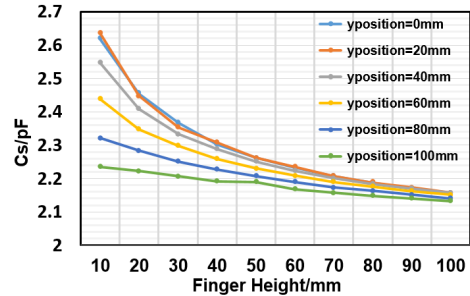


Figure 3: Electrode's self-capacitance versus different finger height.

This illustrates that it is sufficient for the system to determine the Y position by comparing two nearby electrodes' self-capacitances.

2.2 Touch Panel Model

In designing 3D touch sensor systems, it is important to model the touchscreen with co-simulation including the analog front end detection circuitry. A discrete lumped RC model is employed to model the single layer touchscreen shown in Figure 4. To achieve enough accuracy, the long electrode is represented as three lumped units in series, providing an RC constant much smaller than the scanning signal's period. In each lumped unit, C_s represents the electrode's self-capacitance of that particular portion, while C_m represents the coupling capacitance to its nearby parallel electrode. Due to the large sheet resistance of the ITO, typically 10-100Ohm/square [8], an R has been added into the lumped unit to represent the routing resistance. Depending on the position of the lumped unit in the electrode, the value of R , C_s and C_m will be different. The C_s and C_m can be obtained through an EM simulation while the R can be calculated based on the analytical expression below:

$$R = R_s \times \frac{2L}{3(W_u + W_d)} \quad (1)$$

where the R_s is the sheet resistance of the ITO, L is the length of the electrode in Y direction, and W_u , W_d corre-

spond to the upper and lower width of the electrode's in X direction's in each portion, respectively.

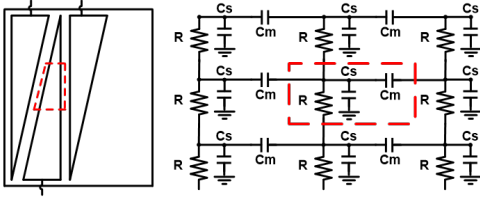


Figure 4: Schematic model of the electrode with the central lumped unit highlighted.

2.3 Hardware Sensing Circuit Design

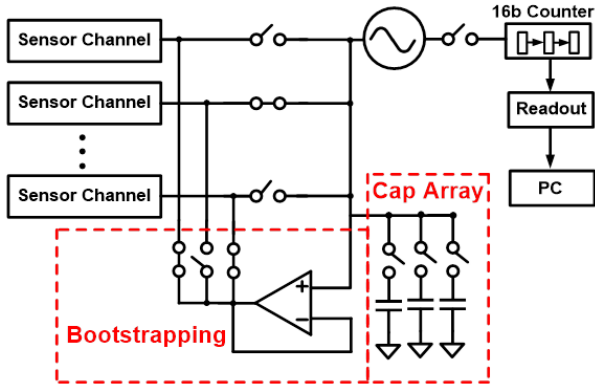


Figure 5: Hardware block diagram of the Airtouch showing oscillator-based capacitive sensing and bootstrapping to eliminate channel coupling.

An overall hardware diagram of the Airtouch system is shown in Figure 5. The hardware circuitry is implemented as described in [3]. The circuit consists of an inverter-based LC oscillator whose frequency is modulated through the loading capacitance. A digital counter tracks the number of periods that the oscillator exhibits in a fixed integration time to estimate the oscillator's frequency. In order to use CDS to reduce the system noise, each channel is trimmed to one fixed reference load value through a capacitor array during initialization. One of the sensor channels is disconnected to the panel and used as the dummy channel. During each measurement cycle, the oscillator is first connected to the active channel and the counter measures the oscillator's frequency. Then it switches to the dummy channel and repeats the measurement. The CDS technique is implemented through outputting the oscillator's frequency difference between the active channel and the dummy channel. Since the dummy channel's load capacitance is equal to the reference load value, any low frequency noise will be suppressed through the subtraction operation and the finger-induced capacitance becomes directly proportional to the frequency difference between these two measurements as derived in (2).

$$C_{finger} = \Delta C = \frac{1}{4\pi^2(f - \Delta f)^2 L} - \frac{1}{4\pi^2 f^2 L} \approx \frac{\Delta f}{2\pi^2 f^3 L} \quad (2)$$

In addition to the oscillator-based CDS sensing, the circuit also implements a bootstrapping circuitry to reduce the inter-channel coupling effect. Although the sensing mechanism is self-capacitive, the large coupling between channels can still create a short path for the signal and cause false detection to occur. For example, when the finger is hovering on one channel, the small fringe capacitance is directly coupled to the other channels through the coupling capacitance which gives an unwanted response on the other channels. To reduce this coupling effect, a tracking amplifier is embedded into the circuit to drive the inactive sensor channels with the same waveform as the active channel one, suppressing the coupling capacitance by enforcing equal potential across the inter-channel coupling capacitors. The proposed Airtouch sensing circuit's die photo is shown in Figure 6, with dimensions and components labeled.

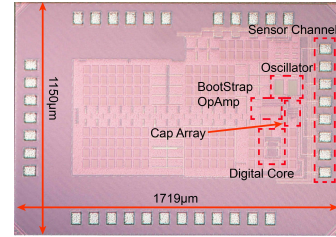


Figure 6: Die photo of Airtouch system.

3. FINGER POSITION ALGORITHM

To reconstruct the finger position effectively, the finger position algorithm has to address several diverse challenges that are not critical in 2D touch sensing, such as extracting position information through much smaller detected finger capacitance, large coupling from other channels and a reduced number of the sensing channels. In addition, the algorithm cannot be too complicated in order to implement within the memory and power limitations of the mobile AP.

To overcome these challenges, a simplified signal flow for the whole backend digital processing procedure is shown in Figure 7. The acquired channel's self-capacitance value first goes to a grouping filter where the unwanted coupled finger capacitance can be filtered out. Then the processed data will be used to calculate X, Y, Z direction position separately. Finally, the finger position in the space will be reconstructed based on the output of the X, Y, Z position with proper smoothing.

3.1 Grouping Filter

As explained above, one of the challenges in the 3D touch sensing is the unwanted channel capacitive response. This unwanted response can be categorized into two main parts: 1. Body-introduced background capacitance; 2. Finger capacitance coupled from other channels. Figure 8 shows how these two mechanisms affect the measurement of the finger position. For example, when the finger is above Channels 1 and 2, Channel 6 may see some fringe capacitance $C_{background}$ due to the hand shape and the coupled active C_{finger} through C_c . This results in inaccurate position estimation. The Grouping Filter aims to exclude these unwanted responses and group the useful channel responses through the following two steps:

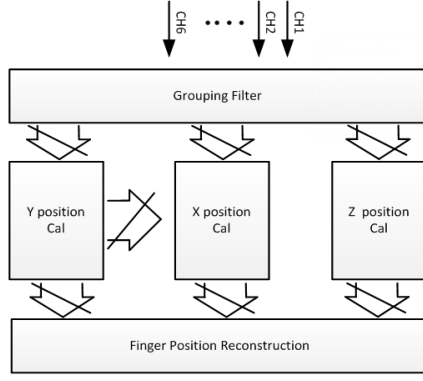


Figure 7: Top block diagram of the Airtouch signal processing showing the finger space position calculation procedure.

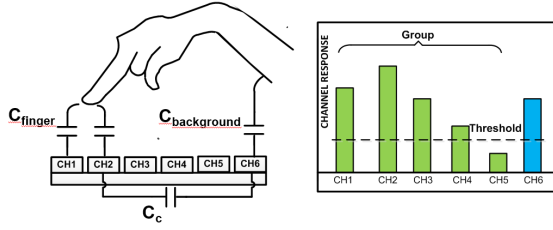


Figure 8: Illustration of the grouping algorithm to filter out unwanted capacitive response.

1. Set a threshold to confirm a valid sensing (channel responses smaller than the threshold will not be regarded as a valid peak response induced by finger).
2. Find the highest peak envelope of the channels' responses and group the corresponding channels.

After grouping, the grouped channels' data will be directly passed to the calculation block while the ungrouped ones will be filtered out.

3.2 Y Position Calculation

The Y position calculation is based on the channel-upper-to-lower ratio (r_{dc}), as defined in Equation 3:

$$r_{dc} = \frac{\sum \Delta C_{upper}}{\sum \Delta C_{lower}}, \quad (3)$$

where the ΔC_{upper} and ΔC_{lower} correspond to each upper and lower triangle channel's sensed finger capacitance as shown in Figure 9. By assuming the sensed capacitance value is proportional to the finger-shielded area, the finger Y position can be derived based on Equation 4:

$$Y_{finger} = \frac{r_{dc} - 1}{r_{dc} + 1} Y_{max}. \quad (4)$$

To further remove the noise effects when one upper or lower channel's response is very small, we add a certain threshold for the r_{dc} . When the r_{dc} exceeds the threshold, the response will be a fixed value. The modified position

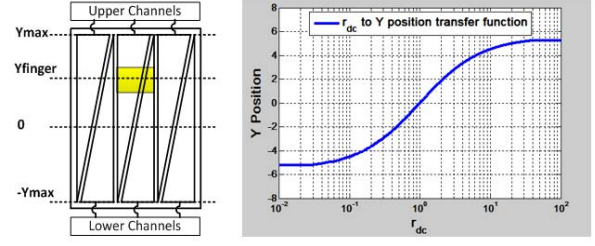


Figure 9: Illustration of Y position calculation: yellow area corresponds to finger position.

equation is described in Equation 5.

$$Y_{finger} = \begin{cases} \frac{r_{dc}-1}{r_{dc}+1} Y_{max} & 0.025 \leq r_{dc} \leq 40 \\ 0.95 Y_{max} & r_{dc} > 40 \\ -0.95 Y_{max} & r_{dc} < 0.025 \end{cases} \quad (5)$$

3.3 X Position Calculation

The X position is estimated based on the center-weighted algorithm. The algorithm can be separated into two parts:

1. Find each electrode's center $X_{position}$ based on the finger's Y position obtained above.
2. Calculate the weighted average of all the electrodes' center $X_{position}$ with their finger capacitive responses and output the average as the final X position.

Each electrode's center $X_{position}$ can be calculated with Equation 6 and the final X position can be derived with Equation 7.

$$X_{center-i} = \frac{X_{top-i} + X_{bot-i}}{2} + \frac{X_{top-i} - X_{bot-i}}{2} \times \frac{Y_{finger}}{Y_{max}} \quad (6)$$

$$X_{finger} = \frac{\sum_i X_{center-i} \times \Delta C_i}{\sum_i \Delta C_i} \quad (7)$$

Here $X_{center-i}$ is the i channel's center $X_{position}$ at the certain Y finger value; X_{top-i} corresponds to the i channel's top-edge's middle point X position; X_{bot-i} represents the i channel's bottom-edge's middle point X position and ΔC_i is the sensed i channel's finger capacitance. These parameters are explained in Figure 10.

3.4 Z Position Calculation and Finger Space Position Reconstruction

The Z position calculation is based on the measured coupling capacitance between the finger and the touch panel. As the size of touch panel is much larger than the user's finger, the coupling capacitance will include both parallel coupling capacitance and fringing capacitance. Here the parallel coupling capacitance is inversely proportional to finger height, while the fringing capacitance has a non-linear transfer function to finger height [9].

To obtain an accurate relationship between the capacitance and finger distance, we have used the 2nd order polynomial curve to fit the EM simulation results on the finger height versus channel's sensed finger capacitance. The 2nd

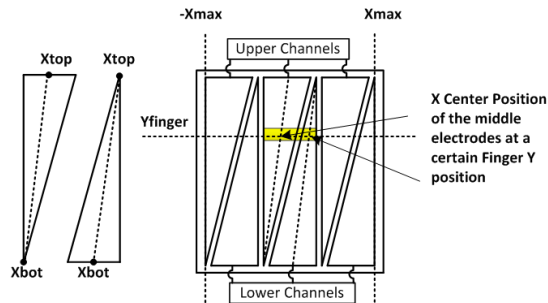


Figure 10: Electrode’s center position calculated at a certain finger Y position.

order polynomial equation can be written as Equation 8:

$$Z_{finger} = \frac{\epsilon_0 A}{a \sum_i \Delta C_i} + \beta \left(\frac{\epsilon_0 A}{a \sum_i \Delta C_i} \right)^2, \quad (8)$$

where α, β are constant coefficients obtained through curve fitting on the EM modelling result, A represents the finger surface area and ΔC_i corresponds to i channel’s sensed finger capacitance. After Z position calculation is done, the X, Y, Z position is passed through a five-tap low pass IIR filter to further smooth the position.

4. EXPERIMENT AND DISCUSSION

4.1 Experimental Result

To demonstrate the operation of the Airtouch 3D touch sensing system, a prototype has been built and set up as shown in Figure 11. The system contains a mobile phone sized ITO touchscreen described above, a low power capacitive sensing circuit to sense the finger capacitance, an ARM-based microprocessor unit (MCU), and a laptop to calculate and display the reconstructed finger position.

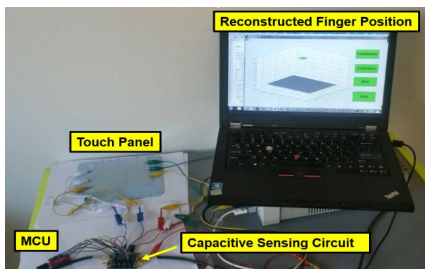


Figure 11: Airtouch demo setup.

The reconstructed finger position is represented as a 1cm^2 green square in the coordinate system, while the touch panel is modeled as a grey rectangle with the same size as the real panel. The system is updated in real time with a sampling speed up to 30 times per second and a power consumption of 2.3mW (this does not include the ARM processor as it can be replaced by mobile AP in a real product environment). The experiment is conducted with a finger hovering above the screen and moving both horizontally and vertically. Figure 12 compares the real finger position with its reconstructed value in the Airtouch system. The video

Table 1: Specifications of the Airtouch System

Airtouch Sensing System	
Application	3D Finger Position Detection for mobile devices
Sensing Approach	Capacitive Sensing
Sensing Channels	6
Touchpanel Size	6 cm × 10 cm
Supply Voltage	1 V (sensing circuit) 3.3 V (MCU)
Power Consumption	2.3 mW
X,Y direction resolution	<1 cm @ 1 cm Finger Height
Z direction resolution	<2 cm@up to 6 cm

demonstration provided in [10] shows the experiment where the finger is moved across the screen, and a video of Matlab reconstruction is provided in [11]. The synchronous finger position captured by the demo with software interface is shown in [12].

The experiment shows that the system achieves an X, Y direction resolution up to 1cm (measured at a finger height at 1cm) and Z direction detection range up to 6cm with a resolution of 2cm . The degradation of Z direction resolution occurs when the finger heights are more than 3cm due to finger modelling inaccuracy. However, at this range, the interface will only require detection of movement gestures instead of accurate height estimates. Table 4.1 lists the characteristics of the demonstrated Airtouch system.

4.2 Discussion

As demonstrated, the Airtouch system offers the potential to improve traditional 2D mobile touch sensing with 3D sensing capabilities. Unlike other reported 3D touch sensing works [6, 13] which are reliant on much larger touch panels and more power consumption, this demonstration focuses on detecting the 3D finger position with minimum power consumption and uses a mobile-screen sized touch panel to enable the compatibility with current smartphone devices. While the prototype Airtouch system employs an oscillator-based-capacitive sensing circuit and customized single-layer touch panel, they can be replaced by any existing high resolution capacitive sensor and existing mobile 2D touch panel.

5. CONCLUSIONS AND APPLICATIONS

In this paper, we propose and successfully demonstrate a single-layer 3D touch sensing system to enable remote finger position detection for mobile device. The proposed touch panel is implemented in single layer to achieve low production cost. Additionally, the low power capacitive sensing methods enable compatibility with existing mobile device environments. Finally, we propose a supporting algorithm that is used to filter out background noise and calculate the finger space position. Our experiment shows the Airtouch system can achieve a 1cm horizontal resolution and a 6cm vertical detection range.

As a new HMI for mobile device, one potential application for the demonstrated Airtouch system is to perform gesture recognition in small-sized electronics. Gesture recognition technology has been commercialized in large television and monitor displays by using its front camera, however it has not been implemented in the mobile device (e.g. Smartphones and Tablets) due to its high power consumption of

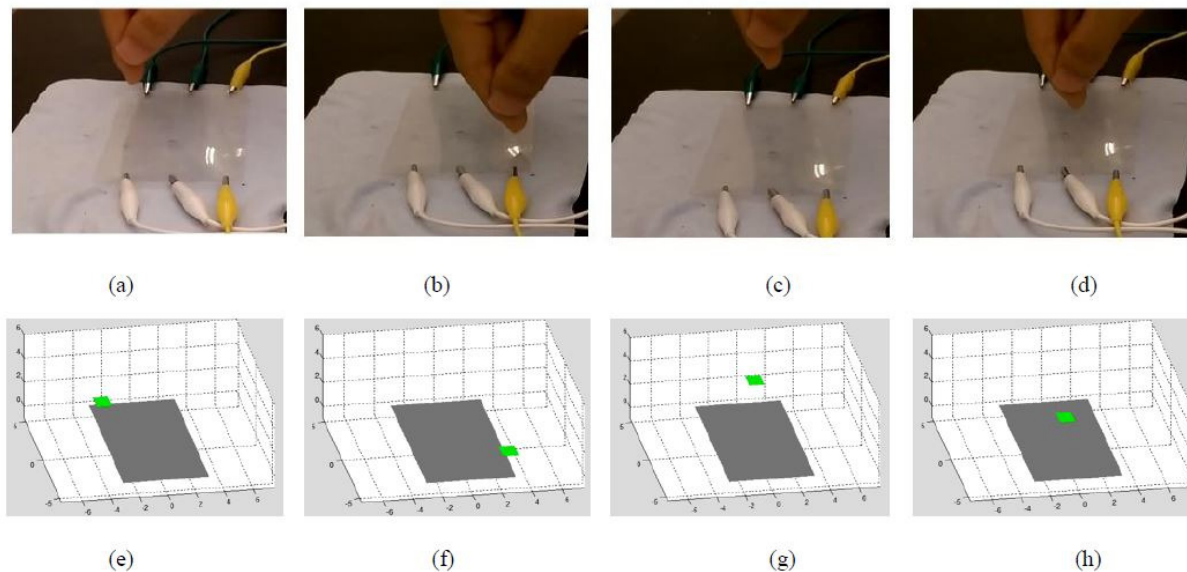


Figure 12: Comparison of Airtouch sensing results versus real finger position. (a), (b), (e), (f) show the finger horizontal moving comparison. (c), (d), (g), (h) show the finger vertical moving comparison .

image processing. Moreover, the emerging wearable devices can also benefit from this technology by implementing the gesture recognition on their small displays. For example, instead of clicking the button on the Apple watch, one can give a rising hand gesture above the screen to control the watch.

For further impact, this system can be used as another sensing methodology for advanced human interactive games in both TV and mobile device. In the current machine vision (optical sensing) approach, camera-based interactive games (e.g. Xbox, Playstation), require a clean stable background behind the user in order to recognize the user's motion effectively which limits the applicable environments. For Airtouch, which senses body-induced capacitance, a stable background is not necessary. By combining the machine vision and Airtouch sensing, smart devices can greatly improve the system sensing accuracy as well as reducing the sensing criteria to provide a better user experience.

6. ACKNOWLEDGMENTS

The authors are grateful to TSMC for foundry support and Wintek Corporation for providing a touchscreen sample.

7. REFERENCES

- [1] I. Statista, "Global smartphone shipments forecast 2010-2019," Link: www.statista.com/statistics/263441/global-smartphone-shipments-forecast/.
- [2] N. Bérci and P. Szolgay, "Towards a Gesture based Human-Machine Interface: Fast 3D Tracking of the Human Fingers on High Speed Smart Camera Computers," in *Circuits and Systems, 2009. ISCAS 2009. IEEE International Symposium on*. IEEE, 2009, pp. 1217–1220.
- [3] L. Du, Y. Zhang, F. Hsiao, A. Tang, Y. Zhao, Y. Li, Z.-Z. Chen, L. Huang, and M.-C. F. Chang, "A 2.3mW 11cm-Range Bootstrapped and Correlated Double Sampling (BCDS) 3D Touch Sensor for Mobile Devices," in *Solid-State Circuits Conference-(ISSCC), 2015 IEEE International*. IEEE, 2015, pp. 1–3.
- [4] G. Barrett and R. Omote, "Projected-capacitive touch technology," *Information Display*, vol. 26, no. 3, pp. 16–21, 2010.
- [5] S. N. Makarov and G. M. Noetscher, *Low-frequency Electromagnetic Modeling for Electrical and Biological Systems Using MATLAB*. John Wiley & Sons, 2015.
- [6] "Microchip: MGC3130 datasheet," Link: www.microchip.com/wwwproducts/devices.aspx?product=mgc3130.
- [7] Z. Tan, S. H. Shalmany, G. Meijer, and M. A. Pertijs, "An Energy-Efficient 15-Bit Capacitive-Sensor Interface Based on Period Modulation," *Solid-State Circuits, IEEE Journal of*, vol. 47, no. 7, pp. 1703–1711, 2012.
- [8] "VLSI Standards Inc, ITO Sheet Resistance Standards," Link: www.vlsistandards.com/products/electrical/ito.asp?sid=86.
- [9] G. Carlson and B. Illman, "The circular disk parallel plate capacitor," *American Journal of Physics*, vol. 62, no. 12, pp. 1099–1105, 1994.
- [10] "Airtouch demo: Raw video," Link: youtu.be/bs3zioGgmWQ.
- [11] "Airtouch demo: Reconstruct model in the matlab," Link: youtu.be/vbeckVDV9v0.
- [12] "Airtouch demo with software interface," Link: youtu.be/x0xgKJwmGWU.
- [13] Y. Hu, L. Huang, W. Rieutort-Louis, J. Sanz-Robinson, S. Wagner, J. C. Sturm, and N. Verma, "3D Gesture-Sensing System For Interactive Displays Based on Extended-Range Capacitive Sensing," in *Solid-State Circuits Conference Digest of Technical Papers (ISSCC), 2014 IEEE International*. IEEE, 2014, pp. 212–213.